ORIGINAL ARTICLE

Perceptual Decisions Recognition in Healthy Individuals Using Electroencephalogram Signals

Ali Barzegar Khanghah [1,2], Zahra Tabanfar [1], Farnaz Ghassemi [1*]

[1] *Department of Biomedical Engineering, Amirkabir University of Technology (Tehran Polytechnic), Iran*

[2] *Institute of Biomaterials and Biomedical Engineering, University of Toronto, Canada*

*Corresponding Author: Farnaz Ghassemi

Email: ghassemi@aut.ac.ir

Received: 21 June 2023 / Accepted: 28 October 2024

Abstract

Purpose: Making a decision based on available sensory information is called "Perceptual Decision-Making". Since the uncertainty and difficulty in individuals' perceptual decision-making can create many adverse effects in their personal and social lives, research in this field seems necessary to achieve a more comprehensive understanding of the brain during perceptual decision-making. Despite numerous studies in this field, no robust system can objectively recognize people's perceptual decisions. This study investigates healthy individuals' Electroencephalogram (EEG) signals during a perceptual decision-making task to fill this research gap.

Materials and Methods: The research employs an online EEG dataset based on visual stimuli, including faces and cars, obtained from 16 participants. After preprocessing the EEG signals, 26 features were extracted from the signals to explore the impact of coherence and spatial prioritization of stimulus on the decision-making process using Friedman's non-parametric statistical analysis. Then, a Fuzzy Radial Basis Function (FRBF) network with the extracted features from TP9 and TP10 channels as input was utilized to classify the data based on the uncertainty of the processes in the brain.

Results: The statistical analysis revealed that differences in the coherence of the stimulus representations have a significant (P-value < 0.05) greater impact on an individual's decision-making process than spatial prioritization. Also, the FRBF network classifier achieved an accuracy of 90.3% in classifying the test data as either a "Face" or "Car.

Conclusion: The classification accuracy results showed that the proposed method is an effective procedure for recognizing human decisions.

Keywords: Perceptual Decisions-Making; Electroencephalogram Signals; Statistical Analysis; Fuzzy Radial Basis Function.

DOI:

1. Introduction

Perceptual decision-making refers to selecting a choice from a list of options based on sensory information. The brain interprets this sensory information into a behavior, and the individual ultimately executes the decision [1-3]. Perceptual decision-making has a prominent place in personal relationships in addition to conscious and cognitive decisions made by individuals. Decisions should be made by considering all relevant evidence [2, 4]. Complex or uncertain decisions may have irreversible consequences for an individual's personal and social life. Studies on Electroencephalography (EEG) have shown that an increase in the activity of the centro-parietal electrodes has been linked to the decision-making process [5].

Heekeren *et al.* [6] describe a general process in the human brain that occurs during perceptual decision-making. Based on the single-cell recordings, the output of different groups of lower-level and selectively tuned sensory neurons can indicate a general mechanism in which higher-level brain regions make perceptual decisions. In this research, the existence of a mechanism in the human brain similar to monkey brains (previous studies) and active brain areas in situations related to more complex decision-making was investigated using fMRI data during a task in which the participant must determine if the displayed stimulus is a human or home image. According to the findings, there are different neurons in brain regions, each of which responds independently to the house and face stimuli, and the individual's decision is the product of the signal of these two groups of neurons. If more neurons signal for the house stimulus, the brain finally identifies it as the house and not the face and vice versa. According to research in [7], the N170 event-related potential can be a powerful indicator for identifying and distinguishing visual stimulus images with a human face from other images. This is because N170 event-related potential has been observed in visual tasks in which one of the stimuli is a human face image. It is also believed that N170 is the product of the brain's early decoding in dealing with the picture of the human face. The N170 component has the greatest amplitude in the lower occipital lobes and typically occurs between 130 and 200 milliseconds [7]. This information becomes helpful in this study as almost half of the dataset consists of human face photos.

So far, neuroimaging methods such as functional Magnetic Resonance Imaging (fMRI) and electroencephalography have been used to study brain activity during decision-making [1, 8]. Electroencephalography is an affordable, non-invasive, and safe modality for brain research. EEG signals reveal physiological aspects of the brain that structural imaging techniques may not reveal. Owing to their high temporal resolution, they can also represent rapid neuronal changes and events in the millisecond scale [9]. Thus, besides being a disease [10] disorder [11] detection or brain-computer communication [12] tool, EEG is often used to explain a variety of brain states, including mental load, arousal, and valence, all of which influence decision-making explicitly or implicitly [1, 13]. Philiastides *et al.* [14, 15] have used EEG analysis and fMRI to obtain non-invasive neural measures of perceptual decision-making. According to their claim, the decision-making process requires at least two general stages of neural processing. The first stage involves presenting evidence to primary sensory areas (for example, a visual experiment involves presenting a stimulus that the eye can perceive). The next step is to collect evidence relevant to the decision to bring it to the decision threshold. The results of [14] revealed the presence of two distinguishing components, the first of which was consistent with the well-known component N170, which is often seen in response to face image stimuli. The second component, more consistent with the research's psychological function, appears at least 130 milliseconds later than the previous component. Their findings indicate that the less evidence there is in the cognitive task, the later the presence of the second component (rather than the first component) occurs. They, in their later research [15], demonstrated that the sequence of events related to perceptual decision-making extends widely throughout the brain neural network, with the lateral occipital complex being one of the most important since it is thought to be the first region in the brain where decision-making occurs. Yajing *et al.* [2] proposed the Discriminative Spatial Network Pattern (DSNP) model, which is an EEG-based computational intelligence structure capable of predicting participant decision-making responses. DSNP features were extracted from the measured brain network during a

single-trial experiment and used to train a Linear Discriminate Analysis classifier (LDA) to predict trial-by-trial responses. Brain signals were recorded from two separate and independent groups using two different EEG systems to evaluate the proposed DSNP method. The trial-by-trial predictors performed efficiently, with an accuracy of 0.88±0.09 and 0.90±0.10 for the first and second datasets, respectively. Imani *et al.* [16] used a hidden semi-Markov model to characterize the decision-making building blocks, assigning each sample to one stage and determining the transition timing between them. They utilized an online available EEG-fMRI dataset, in which participants classified items in a 2x2 factorial design task with internal user state (spatial prioritization) and external world state (stimulus coherency) factors. The findings revealed that the coherency factor, rather than spatial prioritization, influences evidence accumulation for decision-making.

The uncertainty and difficulty in individuals' perceptual decision-making can adversely affect their personal and social lives. Therefore, research in this field seems necessary to understand the brain better during perceptual decision-making. Researchers hope to develop a tool for predicting such human decisions by better understanding the perceptual decision-making process. Although several studies have been conducted in this area, the mechanism of the brain during perceptual decision-making is not yet clear to researchers. Furthermore, previous studies have shown that using neural networks to identify different classes based on EEG signal features can outperform conventional classifiers. To fill this research gap, this study aims to explore EEG signals in healthy individuals while performing a perceptual decision-making task using a Fuzzy Radial Basis Function (FRBF) network. The primary hypothesis of this study is that the fuzzy clustering in this classifier model is similar to what occurs in the brain. Since there is no binary decision-making mode in the brain and there is uncertainty in which each option has a special weight in decision-making and finally, the option that passes a threshold is selected, it has been attempted in this research to incorporate this uncertainty into the final model so that the performance of the perceptual decision recognition system will improve. All in all, this study tends to investigate the separability of two different perceptual decisions made over a visual stimulus, focusing only on the EEG signal. The findings of this research will potentially aid in gaining a better understanding of the neural basis of human perceptual decision-making. Moreover, the results of the proposed classification will demonstrate the capability and capacity of such approaches for integration with Brain-Computer Interface (BCI) systems.

2. Materials and Methods

2.1. EEG Signal

A 62-channel EEG signal from 16 participants was used in this research [17], with a 5 kHz sampling frequency. It is noteworthy that sample size determination was based on the available data, rather than through conventional sample size calculation methods. Electrocardiogram (ECG) and Electrooculogram (EOG) signals related to the electrical activity of the heart and eyes, respectively, were recorded simultaneously on two different channels. The signal also included indicators for different events. Behavioral, EEG, and fMRI data were collected from participants performing visual perceptual decision-making tasks. The recorded EEG signals were divided into two parts of recorded EEG inside and outside the fMRI machine. The data recorded outside the fMRI device was used in this research. Therefore, the EEG signals weren't affected by any MR artifacts. The fMRI data was not used in this research, as most BCI machine learning techniques rely on EEG rather than MRI data. Furthermore, from the computational perspective, a machine learning model based on EEG 1-D signals is more efficient than a model using 2-D MRI data. This is because the input data's dimensionality affects the machine learning models and neural networks' complexity and performance. Higher dimensions require more layers, neurons, and parameters, which increase the computational cost and reduce the learning speed of the model. Additionally, EEG data is more affordable and easier to obtain than MRI data, which facilitates this study's future extension. The presentation of stimulation in this task is visual, and the participants perform the task of perceptual decision-making in a space with 2×2 factors, which include the coherence of the stimuli ("high" and "low" levels) and spatial prioritization ("Yes" and "No"

states). When perceptual decisions are tested in the lab, human participants are typically asked to categorize a particular object stimulus, like an image of a face or a car, into one of two categories [4]. This study's initial stimulus set included 18 car and 18 face pictures. The number of frontal, left lateral, and right lateral views in the two original picture sets was matched. The participant was shown a "Face" or "Car" stimulus with modified spatial phase coherence. As depicted in Figure 1, each experiment began with an arrow in the center of the image, displayed for 1 second. The arrow had three possible states: 1) pointing to the right, 2) pointing to the left, and 3) pointing to both sides. The first two states indicated the location of the stimulus in the next step, while the third state meant that the stimulus would appear randomly on either the right or left side. The participant was instructed to answer quickly and accurately without time constraints.

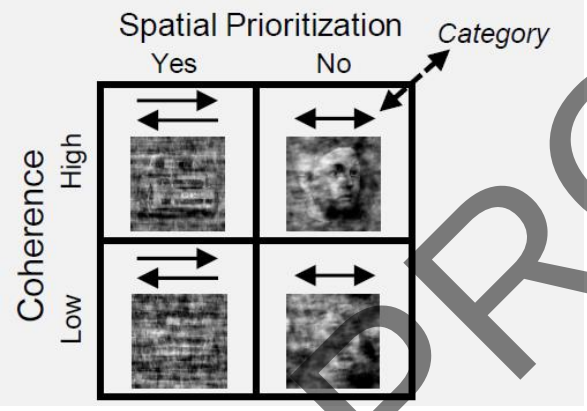

Figure 1. An overview of the study design depicted in [17]. According to this figure, the stimuli presented to individuals in this research included images of "human faces" and "cars," which were classified into four groups based on the two features of coherence (low, high) and spatial prioritization (attention: Yes, No). In the figures with one arrow pointing to the right or left, the person knew where the stimulus would appear in the next step. Otherwise, the stimulus would be randomly displayed on one of the right or left sides

2.2. Preprocessing and Grand Average ERP Calculation

In this study, the raw EEG signals from [17] were used. EEG signal recordings are inherently susceptible to noise and artifacts, meaning that the raw data collected from participants contains not only brain activity signals but also noise and artifacts from physiological (e.g., EOG) and non-physiological sources (e.g., power line interference). To address these issues, we implemented several preprocessing steps: first, we downsampled the signals to 500 Hz to minimize computational load while maintaining necessary frequency resolution; next, we applied average referencing to reduce the impact of potential errors in the reference channel. Baseline correction was performed by subtracting the mean value of each channel from its samples, followed by filtering using a 5^{th}-order elliptic high-pass filter (0.5 Hz cutoff) and a 6^{th}-order elliptic notch filter (50 Hz) implemented with the MATLAB "filtfilt" function to avoid phase distortion. Independent Component Analysis (MULTICOMBI algorithm [18]) was conducted to separate and remove components associated with ocular and cardiac artifacts [19], with components correlated with EOG and ECG channels above a 60% threshold being identified and removed. Signals were then segmented into epochs centered around stimulus presentations, with automatic rejection of epochs exceeding 1000 µV or having a standard deviation greater than five times the channel's standard deviation. Finally, only epochs corresponding to correct participant responses were retained for further analysis, ensuring the validity of features used in subsequent machine learning operations. These preprocessing steps ensured that the final signals were adequately cleaned and ready for further analysis. After that, all individuals' Event-Related Potentials (ERPs) in all stimuli were calculated, and their Grand Averages (GA) in various cases were analyzed. It should be mentioned that only 12 channels of O1, O2, PO3, PO4, PO7, PO8, T7, T8, TP9, TP10, P7, and P8 based on the [7, 17] were considered in the processing steps to reduce the computational load.

2.3. Feature Extraction

The perceptual decision-making task in this research involved human face images. Previous studies have demonstrated that the event-related potential N170 is prominent in visual tasks with human face stimuli [7]. Since the N170 component (120-300 ms) was desired in this study, features were extracted from the signal by considering this component's time interval of occurrence. These features included temporal features such as Latency, Amplitude, Latency/Amplitude ratio, Absolute

Amplitude, Absolute Latency/Amplitude ratio, Positive Area, Negative Area, Absolute Negative Area, Total Area, Absolute Total Area, Total Absolute Area, Average Absolute Signal Slope, Peak-to-Peak (spatial Peak-to-Peak), Peak-to-Peak time window, Peak-to-Peak Slope, Zero Crossing, Zero Crossing Density, Slope Sign Alterations [20] as well as Absolute frequency power of the signal in Delta, Theta, Alpha, Betta and Gamma frequency bands, Spectral Entropy, and Katz Fractal Dimension [21]. A brief explanation per feature is provided in Table 1.

Please refer to [20] for the detailed properties of each feature.

2.4. Statistical Analysis

After extracting these 26 features from 12 selected channels, the statistical differences between the groups under study were examined using existing methods. First, the histogram of each group's data was plotted and analyzed. These plots revealed that the data did not follow a normal distribution. To ensure this, the Kolmogorov-Smirnov test was used to determine the data distribution. In this statistical test, the null hypothesis states that the data distribution follows the normal distribution. If the test result rejects the null hypothesis, then it can be said that the data do not follow the normal distribution, and non-parametric tests must be used to compare different groups. Given the non-parametric distribution of the continuously matched data with more than two groups to compare, the Friedman statistical test followed by a Sidak post-hoc test was used to analyze the presence of significant differences in the study groups based on the data characteristics (non-normal distribution and dependence in the groups).

2.5. Classification

A Support Vector Machine (SVM) is a machine-learning algorithm for classification tasks [22]. The main objective of the SVM classifier is to find the best decision boundary (or hyperplane) that can separate two classes of data with maximum margin. SVMs are effective for datasets with high dimensionality and can also be used for multi-class classification problems. However, the accuracy of SVM classification is mainly for data that can be linearly separated. Another thing that has made this classifier work well, especially for separating the medical data of two classes, is its robustness against outlier data. In general, the effectiveness of this classifier in different tasks depends on the appropriate selection of kernel functions and their parameters. In this study, SVM classification was used as the first classification approach, but ended up with a poor result. Consequently, a more complex alternative, the Fuzzy Radial Basis Function (FRBF) [22], is the final solution.

FRBF network is an artificial neural network that combines the RBF network with a fuzzy c-means algorithm. The RBF network produces a linear combination of radial basis functions for input parameters and neurons as its output. These networks can be used for time series forecasting, classification, and system control. RBF networks usually have three layers: an input layer, a hidden layer with a nonlinear RBF activation function, and an output layer. The network's input is a real-number vector, and its output is a scalar that is a nonlinear function of the input. In this research, for example, the input vector is the features extracted from the previously mentioned channels, and the output is a scalar number representing the final label of the data. A two-step algorithm is typically used to train RBF networks. The vectors of the centers of the radial basis functions in the hidden layer are chosen in the first step. This step in Fuzzy RBF networks uses the Fuzzy C-Mean (FCM) method. Then, in the second training step, a linear model for hidden layer outputs is fitted according to the objective function. Based on the physiological evidence [23], the brain does not make binary decisions but rather deals with uncertainty and assigns different weights to each option. The option that exceeds a threshold is chosen. This research aims to incorporate this uncertainty into the final model to enhance the perceptual decision recognition system's performance. For this purpose, the fuzzy method is applied instead of conventional clustering methods such as K-Means to assign a membership value for each point. This means that, unlike traditional methods that classify each point as either belonging or not belonging to a cluster, the fuzzy method defines a number between 0 and 1 as the degree of membership of each data point to each cluster individually. This results in more reliable final centers.

Table 1. Eighteen morphological features brief explanation

Feature Description	Formula	Feature Description	Formula
Amplitude The maximum signal value. In the formula, $S(t)$ is the value of the signal at the time point t.	$s\,max\{_{max}$	**Total absolute area**	$A_{p\|n\|} = A_p + \|A_n\|$
Latency The time at which the maximum signal value appears.	$t\,t/s(t) = s_{max\,Smax}$	**Absolute total area**	ATAR = $\|A_{pn}\|$
Latency/amplitude ratio	LAR = t_{Smax}/S_{max}	**Average absolute signal slope**	$\left\|\bar{\dot{S}}\right\| = \frac{1}{n}\sum_{t=300ms}^{1000ms-\tau}\frac{1}{\tau}\|s(t+\tau)-s(t)\|$
Absolute amplitude	AAMP = $\|S_{max}\|$	**Peak-to-peak**	$pp = \max\{s(t)\} - \min\{s(t)\}$
Absolute latency/amplitude ratio	ALAR = $\|t_{Smax}/S_{max}\|$	**Peak-to-peak time window**	$t_{pp} = tSmin_{Smax}$
Positive area The sum of the positive signal values	$A_p = \sum_{t=300ms}^{1000ms} 0.5(s(t)+\|s(t)\|)$	**Peak-to-peak slope**	$\dot{s}_{pp} = \frac{pp}{t_{pp}}$
Negative area The sum of the negative signal values	$A_n = \sum_{t=300ms}^{1000ms} 0.5(s(t)+\|s(t)\|)$	**Zero crossings** Zero crossing per the number of times t that S(t) = 0, in the peak-to-peak time window.	$n_{ZC}\sum_{t=t_{Smin}}^{t_{Smax}\Sigma}\delta_S$
Absolute negative area	ANAR = $\|A_n\|$	**Zero crossings density** Zero crossing per time unit, in the peak-to-peak time window.	$d_{ZC} = \frac{n_{ZC}}{t_{pp}}$
Total area	$A_{pn} = A_p + A_n$	**Katz Fractal Dimension** In the formula, L is the sum and d is the average Euclidean distance of the samples from each other.	$D = \frac{log_{10}(L)}{log_{10}(d)}$
Absolute frequency power for Delta, Theta, Alpha, Betta, and Gamma frequency bands. In the formula, the $S(f)$ is the signal value at the frequency f.	$\sum\|S(f)\|^2$	**Spectral Entropy**	$H = -\sum_{m=1}^{N} P(m)\log_2 P(m)$
Slop sign alterations The number of slope sign alterations of two adjacent points of the ERP signal	$n_{sa} = \sum_{t=300ms+\tau}^{1000ms-\tau} 0.5\left\|\frac{s(t-\tau)-s(t)}{\|s(t-\tau)-s(t)\|} + \frac{s(t+\tau)-s(t)}{\|s(t+\tau)-s(t)\|}\right\|$		

3. Results

3.1. Grand Average ERPs

After preprocessing, Grand Average ERPs were calculated and plotted in the 12 channels mentioned above. Grand Average ERPs are the ERPs averaged over a specific channel, and plotting them is a helpful approach for monitoring the variability in ERPs across subjects. These ERPs were calculated and plotted separately for four different states of coherence (low, high) and spatial prioritization (attention; Yes, No) to represent "Face" and "Car" stimuli. Figure 2 shows the Grand Average ERP of the O2 channel for "Face" (part a) and "Car" (part b) stimuli. The blue lines in each plot reflect the "high coherence" with the "spatial priority" state, while the blue dashed lines represent the "high coherence" without the "spatial priority" state. Coherence refers to the noise factor utilized in the function authors in [16] used to add some noise to their pictures. A high coherence means a low noise factor or, equivalently, a high Signal-to-Noise-Ratio (SNR), whereas a low coherence means a low SNR. The red lines reflect the state of "low coherence" with the "spatial priority," while the red dashed lines represent the state of "low coherence" without the "spatial priority". One of the most important components related to ERP analysis is the P300 component. The P300 component is a large positive peak that usually appears around 300 msec after the stimulus onset but can appear up to 1000 msec later [24]. Study [25] has shown that the increment of the P300 component amplitude is associated with post-stimulus processes, such as decision-making. According to Figure 2, the P300 component is observed in all cases with a marginally greater amplitude for "Face" viewing than "Car" viewing. The general waveform of both the "Face" and "Car" groups, on the other hand, follows the same pattern in such a way that in both ERP waveforms (part (a) and (b) of Figure 2), the amplitude of the waveform first increases and reaches a maximum value and then decreases again over time.

According to the Grand Average ERPs, the P300 component is observed in all cases with a marginally greater amplitude for "Face" viewing than "Car" viewing. The general waveform of both the "Face" and "Car" groups, on the other hand, follows the same pattern in such a way that in both ERP waveforms (part (a) and (b) of Figure 2), the amplitude of the waveform first increases and reaches a maximum value and then decreases again over time. The N170 component can also be seen in the waveforms at 130-200 millisecond intervals. This time interval was chosen for feature extraction because of the observation of the N170 component in Grand average ERPs and previous research [7] indicating that this component is typically evoked in response to facial image stimulation. It is worth noting that since the difference in N170 component amplitude between the two classes was more pronounced in the TP9 and TP10 channels, only the features derived from these two channels were used for classification. The grand average ERP for TP9 (part a) and TP10 (part b) is depicted in Figure 3.

3.2. Statistical Analysis

The examination of each group's data distribution by histogram and Kolmogorov-Smirnov test (P-Value < 0.05) revealed that the data did not follow the normal distribution. The results of the Friedman non-parametric test suggest that only three features, Total Area, Zero Crossing, and Slope Sign Alterations, did not show a statistically significant difference between the two classes.

As mentioned before, the images shown to individuals in this study were divided into four categories based on the two features of coherence (low, high) and spatial prioritization (attention; Yes, No). Therefore, the EEG signals of individuals were also categorized into these four related groups. To better understand the differences in brain activity affected by these four types of stimuli, the Sidak post hoc statistical test was utilized to analyze significant differences found by the Friedman test. According to the results, high coherence with spatial prioritization and low coherence without spatial prioritization showed the highest and lowest statistical differences, respectively. In other words, it is inferred from the results that regardless of the attention factor, the test results show significance based on the coherence of the stimulus. As a result, it can be concluded that the variation in the coherence of the stimulus representations significantly impacts the individual's brain mechanism during decision-making.

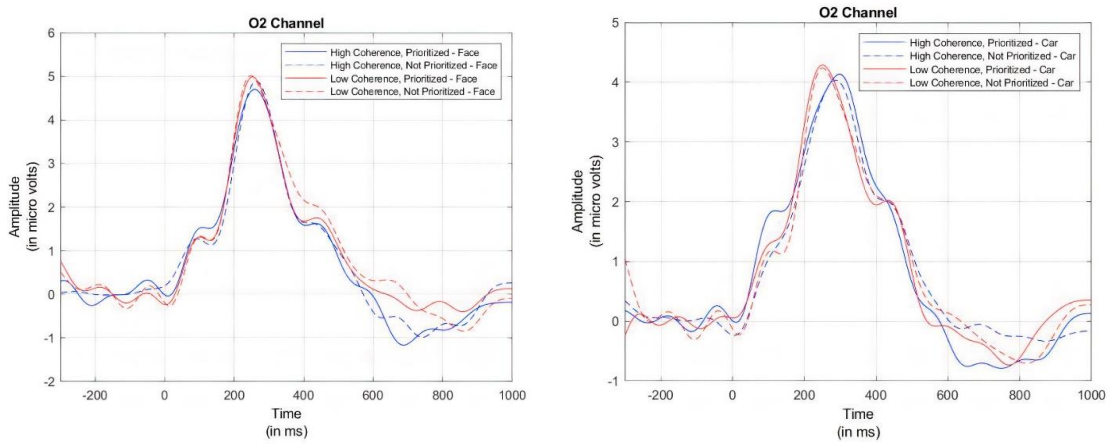

a b

Figure 3. Grand Average ERP of the O2 channel for (a) "Face" viewing and (b) "Car" viewing; The colors blue and red represent High and Low coherence, respectively, while the line (dash) indicates with (without) the spatial priority. According to Figure 2, the P300 component is observed in all cases with a marginally greater amplitude for "Face" viewing than "Car" viewing. The general waveform of both the "Face" and "Car" groups, on the other hand, follows the same pattern in such a way that in both ERP waveforms (part (a) and (b) of Figure 2), the amplitude of the waveform first increases and reaches a maximum value and then decreases again over time

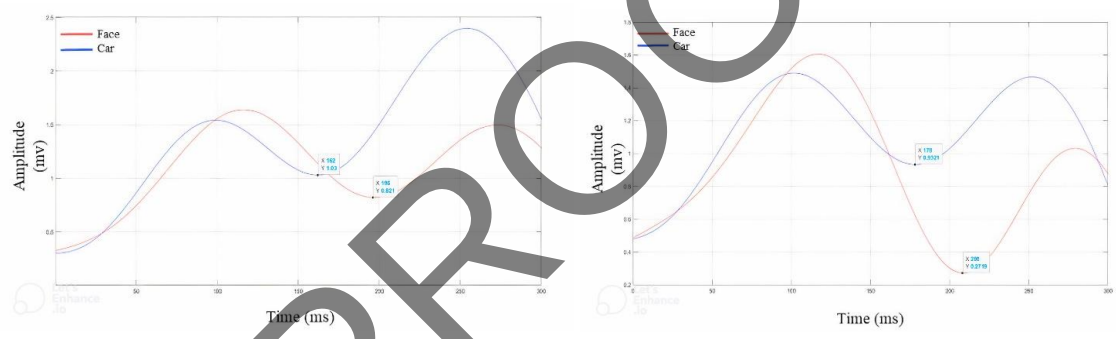

a b

Figure 2. The grand average ERP of channels (a) TP10 and (b) TP9 for the face (Red) vs car (Blue) stimuli

3.3. Classification

Before training the RBF neural network, an SVM with MATLAB's hyperparameter optimization was conducted and validated with the 10-fold cross-validation approach. After fine-tuning, the best model resulted in a test accuracy of 56.9% for the channels TP9 and TP10. The SVM method was dropped because of poor performance. As the computational cost of the fuzzy radial basis function classification is high, training the radial basis function neural network with FCM was performed with only features extracted from two channels, TP9 and TP10. Given that only three features out of 26 showed statistical insignificance, in addition to the large number of data points compared to the number of features, we utilized all 26 features for the classification because the computational cost after feature reduction was negligible. The network's input layer is 26-dimensional data from two channels, the hidden layer is a single layer with 520 neurons (equal to the number of FCM clusters), and the output layer is the data label. We conducted a grid search to find the best parameters for the model. It should be noted that the Fuzzy C-means weighting exponent was set to 2.

In this research, the FRBF network was used for classification. In the FRBF classifier, the number of neurons in the network's hidden layer and, as a result, the number of parameters used is large. Also, the classifier training process includes two stages, leading to a high computational cost for the FRBF classifier. Therefore, unlike the SVM classifier, in the FRBF

classifier, the hold-out method was performed once to evaluate the classifier so that 70% of the data was used for training and 30% for testing. It is noteworthy that these 30% and 70% of the data were chosen randomly, but it was considered that both groups (training/testing) should contain an equal ratio of each of the two classes (face/car). The classification results are shown in the confusion matrix in Figure 4.

The label “0” was used for the face class and “1” for the car class. Figure 4 shows no face picture has been misclassified as a car, whereas a few cars (16.3%) are misclassified as face pictures. Our explanation for this observation is that given the balanced nature of the dataset, the strong N170 occurring in the participant’s signal after seeing the face picture is such a dominant ERP that makes it almost impossible for the model to misclassify face pictures. In contrast, some trials of the car pictures possibly have an almost notable N170 compared to others, leading to their misclassification. Finally, the training accuracy was 92.7%, while the test accuracy was 90.3%. Table 2 shows the results of FRBF network classification for the test data set. According to this table, none of the "Face" samples were mislabeled as "car," while only 9.7% of the "Car" samples were mislabeled as "face.

Table 2. Results obtained from FRBF network classification for classifying "Face” stimulus

$Accuracy_F$	90.3%
$Precision_F$	80.6%
$Sensitivity_F$	100%
$F1\text{-}Score_F$	89.2%

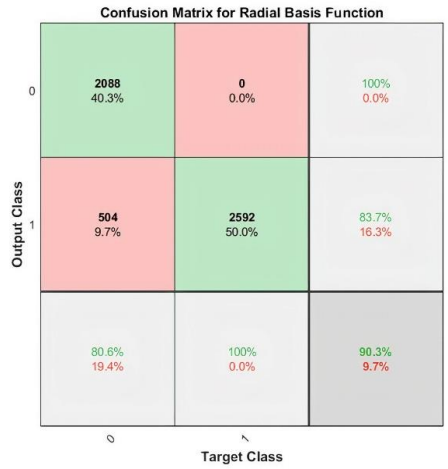

Figure 4. Confusion matrix resulting from the classification using the RBF neural network

4. Discussion

In this study, the brain signals of 16 healthy people were analyzed when performing a perceptual decision-making task to differentiate face images from car images. For this purpose, steps such as preprocessing, investigation of event-related potentials, feature extraction, statistical analysis of feature space, and classification were performed.

4.1. Major Findings

The results of Event-Related Potentials revealed that the P300 component was evident in all of the cases under consideration. Previous research [3] has also revealed the presence of the P300 component in the brain signal during decision-making. According to [26], a higher P300 amplitude demonstrates more confidence in decision-making, whereas a longer P300 latency implies lower attentiveness. Likewise, [27] showed how the P300 amplitude could represent information processing at a preliminary decision-making stage.

The results also showed that the potentials for "Face" observation have a higher amplitude than those for "Car." On the other hand, the general waveform of both "Face” and “Car" stimuli follows the same pattern. The N170 component can also be detected in the waveforms at 130- to 200-millisecond intervals. When observing the facial stimulus, this component has a greater amplitude in the lower occipital regions than the car, consistent with previous research [7] on the relationship between the N170 component and face processing. Based on this, the period of the N170 component activation was used to extract 18 temporal features (out of 26 features) in the following step. In addition, two TP9 and TP10 channels were chosen for feature extraction in the classification process.

Although incorrectly answered epochs were excluded in the preprocessing phase and were not considered in the processing steps, in the end, to have a deeper look at the issue, ERPs related to incorrect answers versus ERPs related to correct answers were also examined. Figure 5 shows the Grand Average ERP of the O2 channel for "correct" answers versus “incorrect” answers. In this case, the amplitude of the P300 component in the Grand Average of event-related potentials in incorrect responses is greater than

in correct responses. This can be due to the person's confidence in selecting the correct answer. For example, it can be presumed that when a person gives an incorrect answer, they have less confidence in their answer. Therefore, their focus is more involved so that they can use the visual evidence they receive from the stimuli to get the two options to the decision threshold and make the final decision. However, this is not in line with the finding in [26] that a higher P300 amplitude indicates more confidence in decision-making. This case has been investigated in a different study [28] using two perceptual decision-making modes with difficult and easy levels. Their findings showed incorrect decisions elicited a larger P300 amplitude in the easy group. In contrast, there was no difference in the P300 amplitude between correct and incorrect decisions in the difficult group. Their findings thus corroborate ours in the simple case.

According to the statistical analysis, the comparison between high coherence with spatial prioritization state and low coherence without spatial prioritization state had the largest number of statistical differences, and the comparison between high coherence without spatial prioritization state and low coherence without spatial prioritization state had the lowest number of statistical differences. As a result, it can be inferred that differences in stimulus representation coherence have a more significant effect on an individual's brain mechanism during decision-making. This finding is in line with the findings of [16], which found that the coherency factor would have a better relationship with the stage of evidence accumulation in the decision-making process rather than the prioritization factor.

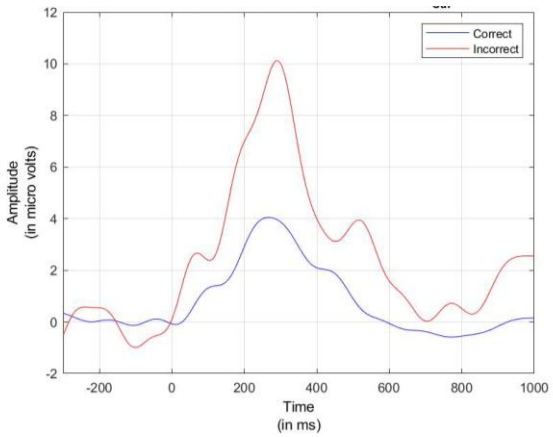

Figure 5. Grand Average ERP of the O_2 channel for "correct" answers versus “incorrect” answers

This research employed a Fuzzy Radial Basis Function (FRBF) network as the classifier. The primary assumption behind this selection is that the fuzzy clustering in this classifier model resembles that can be observed in the brain. To improve the performance of the perceptual decision recognition system, it has been attempted in this research to include uncertainty in the final model since there is no binary decision-making mode in the brain, and there is uncertainty in which each option has a particular weight in decision-making and ultimately the choice that passes a threshold is selected.

Until now, various researchers have investigated perceptual decision-making in humans based on EEG signals. In a study, Pham *et al.* [29] produced a framework for processing EEG data to determine the narrow frequency bands that influence the decision-making process on the same data set. They achieved an accuracy of 66.18% by using the SVM classifier. In another study, Yajing *et al.* [2] proposed the Discriminative Spatial Network Pattern (DSNP) model to predict participant decision-making responses. The Linear Discriminate Analysis (LDA) classifier results on the used EEG signals from two separate and independent groups indicated an accuracy rate of 0.88 ± 0.09 and 0.90 ± 0.10 for the first and second datasets, respectively. The classification accuracy results of the present study (90.3%) showed that the proposed method, which includes feature extraction, channel selection, and FRBF network, is an effective method for recognizing human decisions compared to other state-of-the-art studies. However, the comparison of methods with different datasets may not be fair due to the difference in the nature of the data.

As a practical use of the proposed methodology, individual decision recognition can be applied to smart cars and Brain-Computer Interface (BCI) systems. Designing more reliable and accurate decision recognition systems for these applications can enhance the safety, efficiency, and convenience of human-vehicle interaction.

4.2. Limitations

One of the limitations we dealt with working on this dataset was the small number of available classes. Including only two classes of car and face images,

testing the proposed structure for face images versus more classes using this dataset is impossible. Moreover, there is a low diversity and variability in the image dataset shown to the participants. The dataset does not cover factors like color and the effect of different backgrounds.

4.3. Future Work

We suggest testing the effect of fusing MRI data with the existing EEG data or using MRI data with image processing techniques for classification to compare the results with our study. Moreover, designing a new test comprising more classes covering more aspects like color and background is desirable.

5. Conclusion

Humans sometimes face situations where they must choose between multiple choices provided by sensory information. Uncertainty or disruption in decision-making can lead to serious problems in people's personal and social lives. In this research, the brain signals of healthy individuals while performing a perceptual decision-making task were studied. The results show that the coherency factor had a greater effect on the brain's decision-making process than spatial prioritization. Moreover, the proposed method has a 90.3% accuracy in recognizing a person's decision in a two-class scenario. This study's findings can enhance our understanding of how humans make perceptual decisions in response to visual stimuli, using brain signals and a predictive model.

Acknowledgment

The author(s) received no financial support for this article's research, authorship, and/or publication

References

1- Jacobo Fernandez-Vargas *et al.*, "Subject-and task-independent neural correlates and prediction of decision confidence in perceptual decision making." *Journal of Neural Engineering*, Vol. 18 (No. 4), p. 046055, (2021).

2- Yajing Si *et al.*, "Predicting individual decision-making responses based on single-trial EEG." *NeuroImage*, Vol. 206p. 116333, (2020).

3- Alireza Ettefagh, Farnaz Ghassemi, and Zahra Tabanfar, "Time-Frequency Analysis of Electroencephalogram Signals in a Perceptual Decision-Making Task of Random Dot Kinematograms." *Frontiers in Biomedical Technologies*, (2022).

4- Christopher Summerfield and Floris P De Lange, "Expectation in perceptual decision making: neural and computational mechanisms." *Nature Reviews Neuroscience*, Vol. 15 (No. 11), pp. 745-56, (2014).

5- Jan Herding, Simon Ludwig, Alexander von Lautz, Bernhard Spitzer, and Felix Blankenburg, "Centro-parietal EEG potentials index subjective evidence and confidence during perceptual decision making." *NeuroImage*, Vol. 201p. 116011, (2019).

6- Hauke R Heekeren, Sean Marrett, Peter A Bandettini, and Leslie G Ungerleider, "A general mechanism for perceptual decision-making in the human brain." *Nature*, Vol. 431 (No. 7010), pp. 859-62, (2004).

7- Guillaume A Rousselet, Marc J-M Macé, and Michèle Fabre-Thorpe, "Animal and human faces in natural scenes: How specific to human faces is the N170 ERP component?" *Journal of vision*, Vol. 4 (No. 1), pp. 2-2, (2004).

8- Marios G Philiastides, Tao Tu, and Paul Sajda, "Inferring macroscale brain dynamics via fusion of simultaneous EEG-fMRI." *Annual Review of Neuroscience*, Vol. 44pp. 315-34, (2021).

9- Christoph M Michel and Thomas Koenig, "EEG microstates as a tool for studying the temporal dynamics of whole-brain neuronal networks: a review." *NeuroImage*, Vol. 180pp. 577-93, (2018).

10- Zahra Tabanfar, Mohammad Firoozabadi, Zeinab Shankayi, and Guive Sharifi, "Screening of Brain Tumors Using Functional Connectivity Patterns of Steady-State Visually Evoked Potentials." *Brain Connectivity*, Vol. 12 (No. 10), pp. 883-91, (2022).

11- Ali Nouri and Zahra Tabanfar, "Detection of ADHD Disorder in Children using Layer-wise Relevance Propagation and Convolutional Neural Network: an EEG Analysis." *Frontiers in Biomedical Technologies*, (2023).

12- Zahra Tabanfar, Farnaz Ghassemi, and Mohammad Hassan Moradi, "A subject-independent SSVEP-based BCI target detection system based on fuzzy ordering of EEG task-related components." *Biomedical Signal Processing and Control*, Vol. 79p. 104171, (2023).

13- Catherine Manning, Eric-Jan Wagenmakers, Anthony M Norcia, Gaia Scerif, and Udo Boehm, "Perceptual decision-making in children: Age-related differences and EEG correlates." *Computational Brain & Behavior*, Vol. 4pp. 53-69, (2021).

14- Marios G Philiastides and Paul Sajda, "Temporal characterization of the neural correlates of perceptual decision making in the human brain." *Cerebral cortex*, Vol. 16 (No. 4), pp. 509-18, (2006).

15- Marios G Philiastides and Paul Sajda, "EEG-informed fMRI reveals spatiotemporal characteristics of perceptual decision making." *Journal of Neuroscience*, Vol. 27 (No. 48), pp. 13082-91, (2007).

16- Elaheh Imani, Ahad Harati, Hamidreza Pourreza, and Morteza Moazami Goudarzi, "Brain-behavior relationships in the perceptual decision-making process through cognitive processing stages." *Neuropsychologia*, Vol. 155p. 107821, (2021).

17- Yasmin K Georgie, Camillo Porcaro, Stephen D Mayhew, Andrew P Bagshaw, and Dirk Ostwald, "A perceptual decision making EEG/fMRI data set." *BioRxiv*, p. 253047, (2018).

18- Petr Tichavsky, Zbynek Koldovsky, Arie Yeredor, Germán Gómez-Herrero, and Eran Doron, "A hybrid technique for blind separation of non-Gaussian and time-correlated sources using a multicomponent approach." *IEEE Transactions on Neural Networks*, Vol. 19 (No. 3), pp. 421-30, (2008).

19- N Gholamipour and Farnaz Ghassemi, "Estimation of the independent components reliability of EEG signal in a clinical application." *Biomedical Signal Processing and Control*, Vol. 65p. 102336, (2021).

20- Ioannis Kalatzis, Nikolaos Piliouras, Eric Ventouras, Charalabos C Papageorgiou, Andreas D Rabavilas, and D Cavouras, "Design and implementation of an SVM-based computer classification system for discriminating depressive patients from healthy controls using the P600 component of ERP signals." *Computer Methods and Programs in Biomedicine*, Vol. 75 (No. 1), pp. 11-22, (2004).

21- Zahra Tabanfar, Seyed Mohammad Firouzabadi, Zeynab Shankaei, Giv Sharifi, Kambiz Novin, and Anahita Zoghi, "Brain Tumor Detection Using Electroencephalogram Linear and Non-Linear Features." *Iranian Journal of Biomedical Engineering*, Vol. 10 (No. 3), pp. 211-21, (2016).

22- Sushmita Mitra and Jayanta Basak, "FRBF: a fuzzy radial basis function network." *Neural Computing & Applications*, Vol. 10pp. 244-52, (2001).

23- Lukas N Groschner, Laura Chan Wah Hak, Rafal Bogacz, Shamik DasGupta, and Gero Miesenböck, "Dendritic integration of sensory evidence in perceptual decision-making." *Cell*, Vol. 173 (No. 4), pp. 894-905. e13, (2018).

24- Amin Behzadnia, Farnaz Ghassemi, Soghra A Chermahini, Zahra Tabanfar, and Athena Taymourtash, "The neural correlation of sustained attention in performing conjunctive continuous performance task: an event-related potential study." *Neuroreport*, Vol. 29 (No. 11), pp. 954-61, (2018).

25- John W Rohrbaugh, Emanuel Donchin, and Charles W Eriksen, "Decision making and the P300 component of the cortical evoked response." *Perception & Psychophysics*, Vol. 15 (No. 2), pp. 368-74, (1974).

26- Aida Azlina Mansor, Salmi Mohd Isa, and Syaharudin Shah Mohd Noor, "P300 and decision-making in neuromarketing." *Neuroscience Research Notes*, Vol. 4 (No. 3), pp. 21-26, (2021).

27- Tian Liu, Yanni Chen, Pan Lin, and Jue Wang, "Small-World Brain Functional Networks in Children With Attention-Deficit/Hyperactivity Disorder Revealed by EEG Synchrony." *Clin. EEG Neurosci.*, Vol. 46 (No. 3), pp. 183-91, 2015/07/01 (2014).

28- Kenta Kimura, Aya Murayama, Asako Miura, and Jun'ichi Katayama, "Effect of decision confidence on the evaluation of conflicting decisions in a social context." *Neuroscience letters*, Vol. 556pp. 176-80, (2013).

29- Minh Bao Pham, Nhi Yen Phan Xuan, Quoc Khai Le, and Quang Linh Huynh, "A Decision-Making Process Analysis Based on Prefrontal Hemispheric Asymmetry." in *International Conference on the Development of Biomedical Engineering in Vietnam*, (2022): *Springer*, pp. 838-56.